



Removal of astrazon blue dye from aqueous media by a low-cost adsorbent from coal mining

Andressa dos Santos^{a,b}, Matheus F. Viante^b, Patricia P. dos Anjos^b, Naiane Naidek^b, Murilo P. Moises^a, Eryza G. de Castro^c, Anthony J. Downs^d, Carlos A.P. Almeida^{b,*}

^aLaboratório de Química de Materiais e Sensores—LMSEN, Universidade Estadual de Maringá, 87020-900 Maringá, PR, Brazil, emails: andy_stos@hotmail.com (A. dos Santos), murilomoises@hotmail.com (M.P. Moises)

^bLaboratório de Pesquisa em Ciências Interficiais, Departamento de Química, Universidade Estadual do Centro-Oeste, 85040-080 Guarapuava, PR, Brazil, emails: matheusviante@hotmail.com (M.F. Viante), patricia_2546@hotmail.com (P.P. dos Anjos), naianenaidek@hotmail.com (N. Naidek), Tel. +55 42 36298331 email: cpoliciano@hotmail.com (C.A.P. Almeida)

^cLaboratório de Materiais e Compostos Inorgânicos, Departamento de Química, Universidade Estadual do Centro-Oeste, 85040-080 Guarapuava, PR, Brazil, email: eryza.castro@gmail.com

^dInorganic Chemistry Laboratory, University of Oxford, Oxford OX1 3QR, UK, email: tony.downs@chem.ox.ac.uk

Received 5 November 2015; Accepted 12 March 2016

ABSTRACT

The aim of this study was to evaluate the removal of astrazon blue (AB) dye from aqueous solution by adsorption on an otherwise despoiling and useless mineral waste obtained from coal mining (MWCM) and how this was affected by calcination. The solid waste, as characterized by elemental and thermogravimetric analyses, X-ray diffraction, infrared spectroscopy, specific surface area measurements and Boehm titrations, was found to be composed primarily of calcite, dolomite, and gypsum. Experiments investigated how adsorption was affected particularly by the conditions of pre-calcination of the waste, and also by the contact time, initial AB dye concentration, pH, and temperature of the aqueous medium. Optimum performance was achieved with waste that had been pre-calcinated at 400°C, MWCM400. The kinetics, equilibrium, and thermodynamics of adsorption for MWCM400 were investigated in detail with results that could be satisfactorily rationalized by a pseudo-second-order kinetic model together with a Langmuir isotherm. On the basis of this model, the maximum adsorption capacities were 74.24, 71.63, and 97.18 mg g⁻¹ at 25, 45, and 65°C, respectively. The thermodynamic parameters indicated an endothermic process, $\Delta H_{\text{ads}}^{\circ} = +64 \text{ kJ mol}^{-1}$, driven by an increasing degree of freedom accompanying the adsorption process, $\Delta S_{\text{ads}}^{\circ} = +186 \text{ J K}^{-1} \text{ mol}^{-1}$. The activation energy, $E_a = +9.5 \text{ kJ mol}^{-1}$, was consistent with adsorbate–adsorbent interactions of a predominantly physical type. The results revealed that MWCM400 is a potential low-cost adsorbent for cationic dye removal from residual waters.

Keywords: Adsorption; Astrazon blue dye; Coal mining waste; Calcination; Isotherms; Kinetics

*Corresponding author.

1. Introduction

Inadequate disposal of effluents from dyeing processes in the textile industry is liable to result in environmental problems due to the large amounts of suspended solids, the intense coloration, and raised temperature levels. The direct disposal of these dye-containing effluents to the aquatic environment is highly visible and may, even in low concentration, reduce the penetration of solar light to the extent of affecting photosynthetic processes of aquatic organisms and the balance of the aquatic ecosystem [1–4]. The dyes may also be carcinogenic and mutagenic, causing severe damage to the human body should they be ingested from drinking water that is not properly treated. The hazards and waste could be avoided were clean water to be recoverable from such effluents, an issue made more acute as the rising population increases the demand for water, suggesting the likelihood of severe competition for safe drinking water in the near future.

Several methods have been developed for dye removal from residual waters. These include flocculation and coagulation [5], membrane separation processes [6], electrochemical techniques [7], reverse osmosis, and aerobic and anaerobic microbial degradation [8]. Most methods are not very effective and are also expensive. In addition, synthetic dyes may be resistant to biodegradation, photodegradation, and oxidation. The adsorption method has been established as an effective and attractive process for dye removal [9–13], being considered an economically realistic option. The adsorbent most widely used for dye removal is granular or powdered activated carbon. This is expensive, however, and needs to be regenerated after use [2–4,14]. There is a problem, too, with the sourcing of the activated carbon which may not come solely from good forest stewardship. An alternative approach is to employ local adsorbents, such as clays, agricultural wastes, ashes, and so on.

Coal extraction from mines in Treviso city, Santa Catarina state, Brazil, generates a kind of mineral waste the discarding of which demands increasing space for storage and causes, through its improper disposal, major pollution problems. This despoiling waste, derived mainly from natural sedimentary strata covering the coal layer about 50 m below the surface, is formed of several compacted minerals. Huge amounts of the waste are produced daily. The manifest problems associated with its accumulation could be reduced if it had any application. That it, or a fraction of it, might be used as an effective alternative to other adsorbents [14] in the treatment of residual waters invites investigation since the textile industry

plays an important part in the economy of Santa Catarina state.

The present paper reports a study seeking to evaluate the adsorption capacity of a fraction of this Mineral Waste from Coal Mines (MWCM) for Astrazon Blue (AB) used extensively in the textile industry for dyeing acrylic fibers, with particular reference to the effects of pre-calcination of the adsorbent. Various physical techniques were deployed to characterize the solid samples. Batch adsorption experiments were then carried out to investigate potentially important influences on the adsorption process and to determine the relevant equilibrium, kinetic, and thermodynamic parameters for the adsorbent showing optimum properties.

2. Materials and methods

2.1. Materials

Samples of MWCM (Fig. 1) were obtained at Esperança Mine (Carbonífera Metropolitana—Treviso, Santa Catarina state, Brazil).

The adsorbate AB FGRL dye, obtained from Quimisa (Brusque, Brazil), was used as received without further purification, being in fact a mixture of two dyes (Fig. 2): C.I. Basic Blue 159 and C.I. Basic Blue 3 (with a mass ratio of 5:1, respectively) [15], both of them cationic dyes with an absorption peak in the visible region centered at $\lambda_{\max} = 600$ nm. The close similarity of these absorption properties necessitated the treatment of AB in effect as a single dye for the purposes of the following adsorption studies. Other chemicals, all of analytical grade, were used without further purification.

2.2. Preparation of MWCM and calcinated MWCM

Firstly, MWCM was ground and sieved (ASTM sieves) in order to select particles with sizes in the



Fig. 1. Mineral waste from coal mining (MWCM).

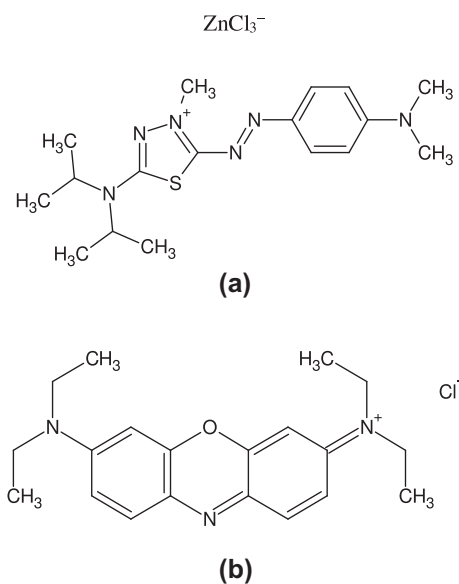


Fig. 2. Chemical structures of (a) C.I. Basic Blue 159 and (b) C.I. Basic Blue 3.

range from 105 to 125 μm . The selected material was washed with distilled water, then dried in a stove at 80°C for 24 h, and stored in sealed flasks for further analysis. This was $\text{MWCM}_{\text{natural}}$.

Separate samples of $\text{MWCM}_{\text{natural}}$ (5.0 g) were each calcinated for 4 h in a muffle at 80°C (MWCM_{80}), 200°C (MWCM_{200}), 400°C (MWCM_{400}), 600°C (MWCM_{600}), and 800°C (MWCM_{800}), and stored. Although similar untreated $\text{MWCM}_{\text{natural}}$ had already been used as an adsorbent for basic dyes [11], a major purpose of the present studies was to determine the effects of calcination of the material at five different temperatures on the adsorption of the AB dye.

2.3. Preparation of solutions

A stock solution of AB dye (2,000 mg L^{-1}) was prepared by dissolving an accurately weighed quantity of dye in distilled water. Working solutions at concentrations of 200, 400, 600, 800, 1,000, 1,200, 1,400, 1,600, and 1,800 mg L^{-1} were prepared by diluting the stock solution with suitable volumes of distilled water.

Buffered AB dye solutions were prepared at pH 3.0 ($\text{KC}_8\text{H}_5\text{O}_4$ 0.1 mol L^{-1} + HCl 0.1 mol L^{-1}), pH 6.0 ($\text{KC}_8\text{H}_5\text{O}_4$ 0.1 mol L^{-1} + NaOH 0.1 mol L^{-1}), pH 8.0 (KH_2PO_4 0.1 mol L^{-1} + NaOH 0.1 mol L^{-1}), and pH 11.0 (Na_2CO_3 0.1 mol L^{-1} + HCl 0.1 mol L^{-1}). Unbuffered AB dye solutions used extensively in our adsorption experiments exhibited initially a pH of 5.5.

2.4. Equipment and characterization

The AB dye concentration was measured using a UV–vis spectrophotometer (Varian Cary 50 spectrophotometer, USA) with a 1-cm path-length cell to monitor the absorbance at $\lambda_{\text{max}} = 600$ nm corresponding to the maximum absorbance of the two cationic dyes. pH measurements were made using a C535 Multi-Parameter Analyzer, Consort. The batch adsorption experiments were carried out on a stirrer having five stirrer shafts (AM5E), where five solutions were simultaneously stirred in separate glass flasks the temperature of which was maintained by a circulating water bath with a hydraulic thermostat controller (521/3D—Nova Ética).

Elemental analysis of $\text{MWCM}_{\text{natural}}$ samples was carried out by energy-dispersive X-ray spectroscopy (EDS) using an electron microscope, low vacuum, Hitachi High Tech TM-3000 coupled to EDS SwiftED-3000, with a tungsten filament and operating at 15 kV.

The different MWCM samples, before and after calcination, were submitted to X-ray diffraction (XRD) analysis on a D2 Phaser Bruker instrument with $\text{Cu K}\alpha$ radiation ($\lambda = 1.5418 \text{ \AA}$), 30 kV applied voltage and a current of 10 mA, the diffraction pattern spanning the range 10–70° (2θ) with a step size of 0.05°, and a scan speed of 1.00° min^{-1} . Mineral phases were identified by the search-match method using the ICDD-PDF2 2009 data base and EVA software.

Fourier transform infrared (FT-IR) spectra for MWCM samples were obtained with a Bruker FTIR spectrometric analyzer, Vertex 70V model, for samples in the form of KBr disks (ca. 1.0 wt.%), with 4 cm^{-1} resolution, 64 scans being averaged over the scan range 4,000–400 cm^{-1} .

The MWCM samples were characterized by thermogravimetric analysis with a Thermogravimetric/Differential Thermal Analyzer (TG-TA instruments Q-50); this covered the temperature range from 25 to 1,000°C at a heating rate of 10°C min^{-1} under an N_2 atmosphere.

The specific surface areas of the MWCM samples were measured using the Brunauer–Emmet–Teller (BET) method. Results were obtained by means of pure liquid N_2 adsorption at 77 K using an ASAP 2020 analyzer, with P/P_0 between 0.05 and 0.03. All samples were degassed under vacuum at 105°C for 12 h prior to analysis.

The total surface acidity and basicity of the MWCM samples were determined by the Boehm method [16]. Suspensions of each sample were prepared by mixing 0.15 g of the adsorbent with 50.0 mL of 0.1 mol L^{-1} NaOH or 0.01 mol L^{-1} HCl standard solutions. The suspensions were stirred for 24 h at

25°C; the samples were then filtered and aliquots of the supernatant solution collected. The excess of acid or base was back-titrated with 0.01 mol L⁻¹ NaOH (total basic groups) and 0.01 mol L⁻¹ HCl solutions (total acidic groups), respectively. Each titration was repeated twice.

2.5. Methods

The batch adsorption experiments were carried out in a set of 80-mL glass cells each containing 1.0 g of MWCM and 50.0 mL of AB dye solution. Each sample was stirred at 450 rpm in a thermostated environment provided by an outer circulating-water bath. Aliquots of 0.1 mL of the AB dye solutions were withdrawn at regular time intervals, and then diluted and centrifuged (Centrifio 80-2B) for 10 min at 2,000 rpm. The absorbance values of the supernatant liquids were then monitored by UV–vis measurements. For each stirred solution, aliquots were collected at appropriate time intervals to follow the rate of color fading by reference to the relevant absorbance values. The concentrations of the solutions were found from the linear regression equation obtained by plotting a calibration curve for the AB dye. The amount of AB dye adsorbed by MWCM was calculated using the following mass balance equation [17]:

$$q_t = \frac{(C_0 - C_t)V}{m} \quad (1)$$

where q_t is the mass of AB dye adsorbed per unit mass of adsorbent at any time t (mg g⁻¹); C_0 and C_t are, respectively, the initial concentration of the AB dye solution and the concentration at any time t (mg L⁻¹); V is the volume of the AB dye solution (0.05 L); and m is the mass of the adsorbent used (1.0 g).

Batch adsorption experiments were carried out for the five calcinated samples of MWCM by stirring 1.0 g of each with unbuffered AB dye solutions (pH 5.5–7.5) at a concentration of 1,000 mg L⁻¹ and a temperature of 45°C to analyze the effects of calcination. Such experiments were subsequently repeated under what appeared to be optimum conditions with a selected sample of calcinated MWCM at two different temperatures of 25 and 65°C.

To study the effects of pH, experiments were carried out with buffered AB dye solutions at pH 3.0, 6.0, 8.0, and 11.0, as well as unbuffered AB dye solution (pH 5.5–7.5). Before each adsorption experiment, the buffered AB dye solution was stored for 10 d to check for possible changes in the maximum absorbance ($\lambda_{\max} = 600$ nm).

3. Results

3.1. Characterization of the MWCM samples

The elemental composition (in weight %) of MWCM_{natural} determined by EDS measurements was found to be as follows: C 11.7, O 43.0, Mg 0.9, Al 0.8, Si 0.4, S 12.4, Ca 26.8, Mn 0.9, Fe 3.2. Calcium was thus the predominant metallic element, supplemented by much smaller amounts of magnesium, aluminum, manganese, and iron, with carbonate and sulfate presumed to be the main anions, but only traces of silicate.

The XRD results (Fig. 3) played a key role in the characterization of the MWCM samples and the changes brought about by calcination. The pattern shown by the material before heat treatment, MWCM_{natural}, was dominated by reflections identifiable with the carbonate minerals calcite (PDF 01-071-1663) and dolomite (PDF 00-36-0426). A weak reflection at 12° (2 θ) suggested also the presence of the sulfate mineral gypsum, CaSO₄·2H₂O (PDF 00-006-0046). At calcination temperatures up to 400°C, the XRD pattern varied but little, although the reflection at 12° disappeared to be replaced by a new weak reflection at 25.7° associated with the formation of a new phase. This reflection grew and further weak reflections associated with the same, common phase appeared with calcination at 600°C. Finally, calcination at 800°C clearly resulted in the disappearance of the carbonate phases and the emergence as primary products of anhydrous calcium sulfate, the source of the reflection at 25.7° (PDF 01-074-1782), and calcium oxide (PDF 01-070-4068). Despite the observation of a number of weak reflections that could not be positively identified (particularly for MWCM800), more detailed characterization was not feasible on this basis. The presence in the solids of several different phases inevitably incurred the risk of masking of reflections from one phase by those from another; in addition, the XRD data could do little for any poorly crystalline or amorphous constituents of the samples [18,19]. Iron may well have been present as carbonate in the form of siderite [20], but the close similarity of its principal reflection to that of dolomite precluded positive identification.

The FTIR spectra of the samples (Fig. 4) served to corroborate these conclusions. Thus, the spectrum of MWCM_{natural} was dominated by a prominent, broad absorption centered at 1,414 cm⁻¹ and sharper, weaker ones at 872 and 713 cm⁻¹ clearly attributable to fundamental vibrations of the CO₃²⁻ ion present in the calcite and dolomite [18,21]. Less prominent, broad features centered at 3,530, 3,400, and 1,120 cm⁻¹ could be attributed to the presence of gypsum [22]. Decay of

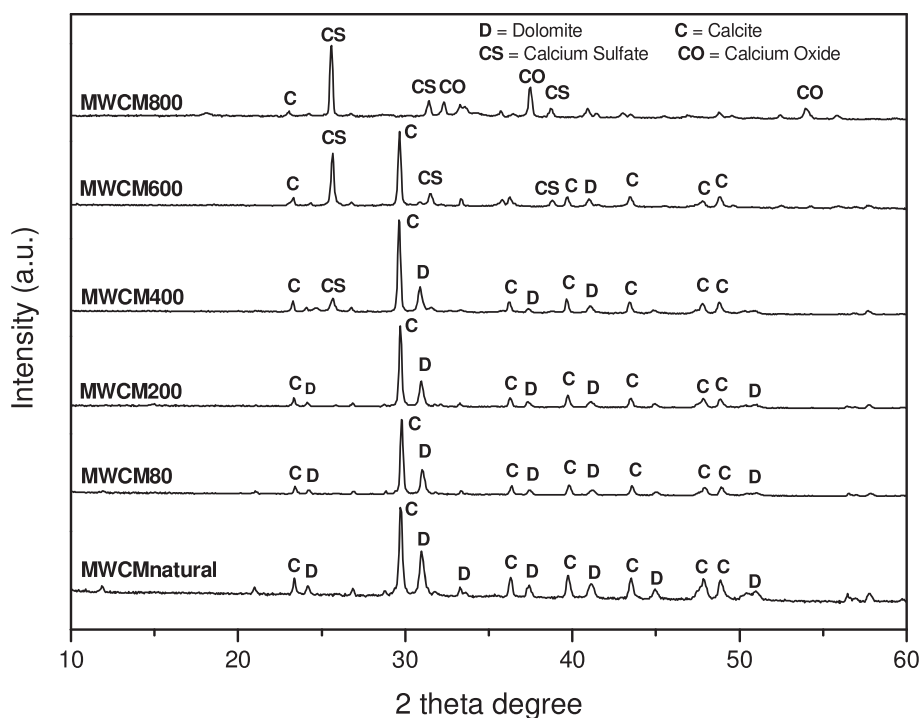


Fig. 3. X-ray diffractograms for natural and thermally treated MWCM samples.

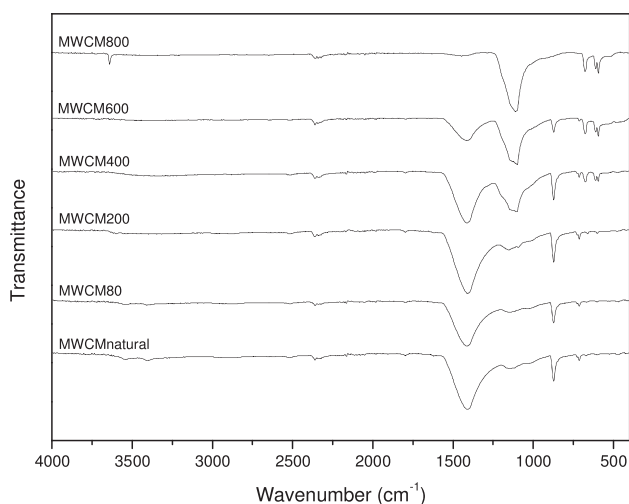


Fig. 4. FTIR spectra of solid MWCM samples.

the carbonate bands witnessed the decomposition of the calcite and dolomite on calcination of the MWCM at progressively high temperature. Simultaneously the band at $1,120\text{ cm}^{-1}$ was observed to grow and with it there appeared for MWCM400, MWCM600, and MWCM800 new bands at 676 and 593 cm^{-1} . All these features can be identified with stretching and bending fundamentals of the SO_4^{2-} ion in anhydrous calcium

sulfate [23,24]. The spectrum of MWCM800 showed an additional absorption band at $3,642\text{ cm}^{-1}$ that must be attributed to O–H stretching modes of $\text{Ca}(\text{OH})_2$ formed from calcium oxide through the adventitious, but unavoidable ingress of moisture while the FTIR measurements were being made [18,21]. Wavenumber shifts of the band centers, notably in the range $1,000$ – $1,500\text{ cm}^{-1}$, were associated with changes of contour as the heat treatment altered the composition of the MWCM. The spectra betrayed no evidence for the presence of any organic or organic-sourced species other than carbonate.

The results of the thermogravimetric measurements (Fig. 5) showed for MWCM_{natural} a gradual weight loss of less than 2% up to temperatures of 400°C associated mainly with the loss of water. The weight loss accelerated as the temperature rose to 600°C with the greatest change coming between 600 and 800°C to give a total loss of ca. 40% of the original mass, to be associated primarily with the evolution of CO_2 from the decomposing calcite and dolomite. The initial presence of adsorbed or coordinated water (in gypsum, for example) was likely to decrease the availability of active sites on the MWCM surface by electrostatic neutralization. On the other hand, thermal treatment at temperatures higher than 400°C produced more dramatic changes of structure and composition,

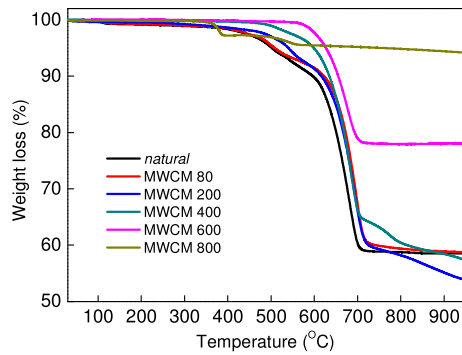


Fig. 5. TG curves for MWCM samples.

with increased crystallization and surfaces assuming a more basic character (with significant implications for a raised pH in any aqueous phase in contact with the solid). These considerations pointed to MWCM400 as the likeliest candidate for optimum adsorption of AB dye.

All the MWCM samples exhibited the low BET surface area (Fig. 6) typical of nonporous materials, this area being localized on the surface of the solids [25]. The MWCM400 sample showed a higher specific surface area ($5.5 \text{ m}^2 \text{ g}^{-1}$) and a higher pore volume ($6.14 \times 10^{-3} \text{ cm}^3 \text{ g}^{-1}$) than any other sample.

The adsorbent surfaces were analyzed by Boehm titration [16,26]. The results (Fig. 7) revealed a higher surface acidity for MCWM400 than for any other sample. Taken with the other properties, this served to confirm MWCM400 as the dye adsorbent of choice.

3.2. Effects of calcination of MWCM on AB dye adsorption

Systematic adsorption experiments showed that the degree of AB dye adsorption varied with the calcination temperature of MWCM (Fig. 8) in the order $\text{MWCM}_{\text{natural}} < \text{MWCM}_{600} < \text{MWCM}_{80} < \text{MWCM}_{800} < \text{MWCM}_{200} < \text{MWCM}_{400}$. The superiority of MWCM400, with an adsorption capacity roughly twice

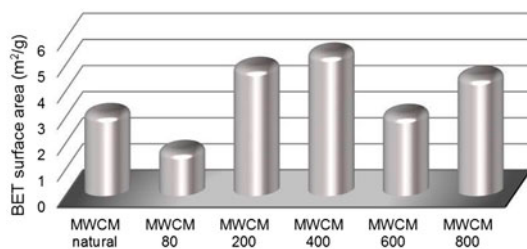


Fig. 6. Specific surface area (BET) for MWCM samples.

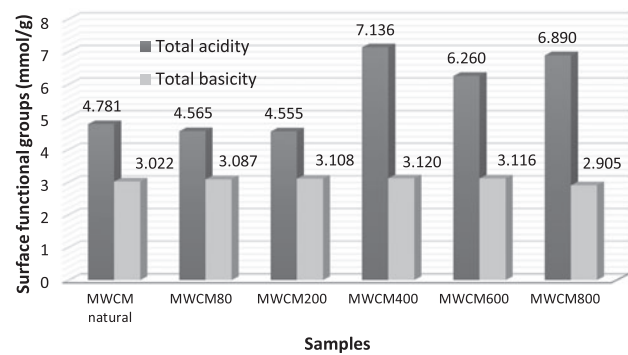


Fig. 7. Boehm titration for MWCM samples.

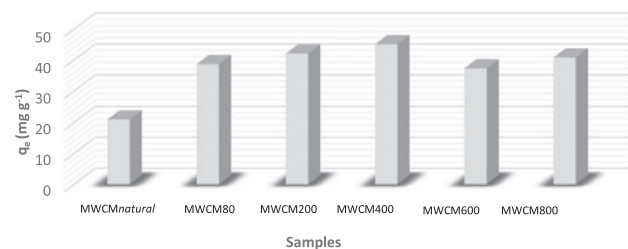


Fig. 8. Effect of calcination of MWCM samples and the mass of AB dye adsorbed at equilibrium: $C_0 = 1,000 \text{ mg L}^{-1}$, temperature: 45°C , and pH 7.3.

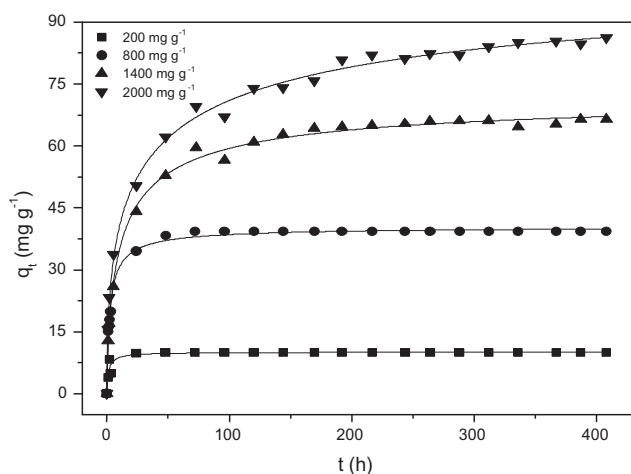
that of $\text{MWCM}_{\text{natural}}$, was not only consistent with the physical properties of the material and the changes that had occurred on its surface, but also made it the obvious adsorbent for all subsequent experiments. As the temperature of calcination of the MWCM was raised, adsorbed and coordinated water molecules were first removed, thereby increasing the active surface area and so the adsorption capacity. For this reason, MWCM400 and MWCM200 displayed a greater adsorption capacity than did the natural samples, while retaining otherwise the crystallinity and main chemical composition of the original material (as confirmed by the XRD measurements). Calcination at temperatures of 600 and 800°C led, by contrast, to radical changes of both form and chemical composition with the progressive decomposition of the carbonate phases.

3.3. Effects of contact time

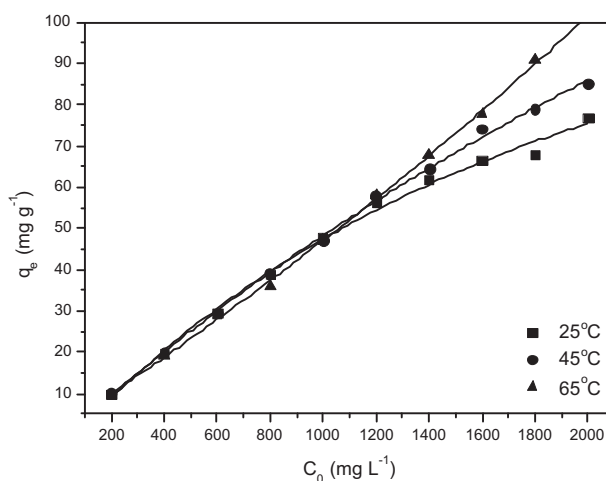
The effect of contact time on AB dye removal by MWCM400 was examined (Fig. 9(a)) for four different initial AB dye concentrations. The higher the initial AB dye concentration, the longer was the contact time needed to reach equilibrium. The rate of adsorption of

AB dye increased rapidly at short contact times and then fell away in a manner related to the initial AB dye concentration. The higher the dye concentration, the more gradual was the slope of the curve before leveling off (after about 300 h) to a steady value implying that the system had come to equilibrium. At low concentration (200 mg L⁻¹), by contrast, equilibrium was reached much more quickly (after about 20 h) because there were relatively many sites on the MWCM400 surface free to accommodate AB dye species with little competition between these species for the available binding sites [27,28]. With increasing concentration (800, 1,400, and 2,000 mg L⁻¹), the AB

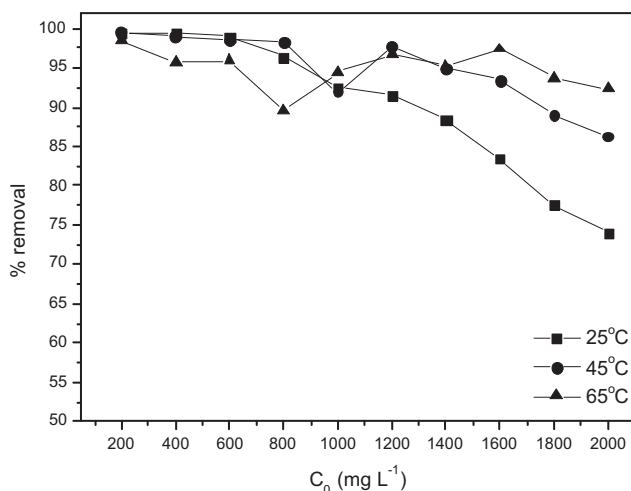
dye species needed to compete for a limited number of binding sites. As more and more adsorbate species occupied the surface sites, moreover, the remaining vacant sites became less accessible by virtue of the repulsion between the adsorbate species. The incoming species were forced to lodge on the adsorbent and then rearrange themselves to accommodate as many as possible, in accordance with the driving force set by the new equilibrium conditions. The resulting rearrangements on the MWCM400 surface accounted then, in part, for the more gradually shelving adsorption curves observed in experiments with more concentrated solutions (1,400 and 2,000 mg L⁻¹).



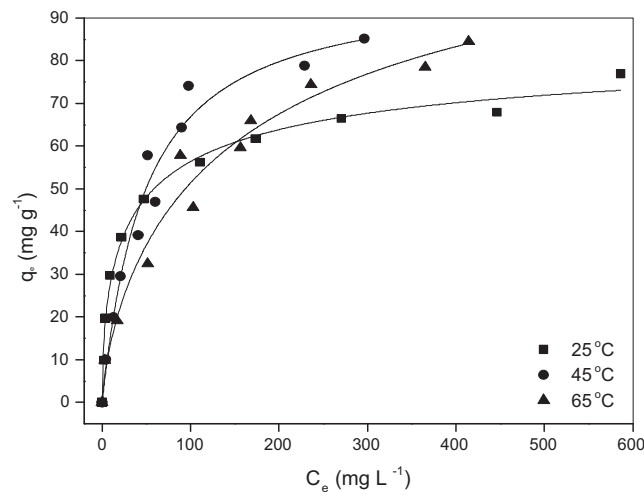
(a)



(b)



(c)



(d)

Fig. 9. (a) Effect of contact time on the adsorption of AB dye onto MWCM400 at 45°C and pH 7.3, (b) effect of initial AB dye concentration on the adsorption of AB dye onto MWCM400 showing the quantity of AB dye removed, q_e , (c) the percentage of AB dye removed, and (d) the isotherms.

3.4. Effects of initial dye concentration

Experiments were also performed to assess how the equilibrium uptake of AB dye was affected by the initial concentration of the dye over the range from 200 to 2,000 mg L⁻¹ (Fig. 9(b) and (c)). The mass of adsorbed dye increased as the initial solution concentration increased while the percentage of removal decreased [29,30]. The adsorption capacity increased as a result of the enhanced driving force associated with the greater concentration gradient subject, that is, to the availability of active sites on the adsorbent. The decreased percentage of removal attending the rise in AB dye concentration reflected the compromising of the uptake of adsorbate by competition between ever more species for a limited number of active sites and by interaction between these species once adsorbed.

3.5. Effects of pH

Varying the initial pH between 3.0, 6.0, 8.0, and 5.5–7.5 (unbuffered solution) caused the uptake of adsorbed AB dye to change from 77.2 to 71.0, 59.3, and 89.4%, respectively. Optimum removal of AB dye onto MWCM400 was thus achieved in the unbuffered solution. Increasing the pH inevitably favored retention of the cationic dyes in the solution phase, whereas reducing the pH beyond a certain level was likely to result in competition between these dyes and H₃O⁺ ions for the negatively charged sites on the adsorbent. That the unbuffered solution should give the best results hinted too at the possibility of competition between the cations of the buffering agent and the AB dye cations for the active sites.

3.6. Effects of temperature

The effects of changing the temperature of the solution on AB adsorption and the percentage uptake of the dye were investigated (Table 1). In general, both the amount and the percentage of dye adsorbed increased as the temperature rose from 25 to 65°C. That higher temperature favored AB dye removal implied kinetic control of adsorption in an endothermic process. The increased uptake was probably due to the higher diffusion rate of the adsorbate ions made possible by the reduced viscosity of the solution [13]. The results of these experiments were analyzed for the information they gave about the kinetics, the adsorption isotherm, and the thermodynamics of the adsorption process.

4. Discussion

4.1. Kinetic properties

When an adsorbent is added to a solution containing an adsorbate, adsorption proceeds at a rate strongly influenced by the physicochemical conditions under which the process is performed including, for example, the reactivity of the solid surface in relation to the adsorbate and the natures of the other species present in solution [31].

In the present study, different models describing the adsorption capacity of the adsorbent in liquid/solid systems have been examined. Firstly, the equations of pseudo-first-order [32] and pseudo-second-order [33–35] kinetic models were applied to evaluate the rate of adsorption. The respective Eqs. (2) and (3) are:

$$\ln(q_e - q_t) = \ln q_e - k_1 t \quad (2)$$

$$\frac{t}{q_t} = \frac{1}{k_2 q_e^2} + \frac{t}{q_e} \quad (3)$$

where q_e is the mass of AB dye adsorbed at equilibrium (mg g⁻¹), t the time (h), k_1 the rate constant of a pseudo-first order (h⁻¹), and k_2 the corresponding constant of a pseudo-second-order process (g mg⁻¹ h⁻¹).

The parameters appropriate to the two models (k_1 , q_e , r_1 and k_2 , q_e , r_2) have been determined from plots of $\ln(q_e - q_t)$ vs. t and t/q_t vs. t , respectively (Table 1). The values of r_1 and r_2 indicate that the experimental results are better described in terms of a pseudo-second order [36,37] than of a pseudo-first-order kinetic model at the three temperatures studied. Such a conclusion is reinforced by the values of q_e calculated for this model which are more consistent with the experimental findings.

Adherence to a pseudo-second-order model might suggest that the adsorption takes a chemical form [38]. As the adsorption phenomenon is such a complex process, however, it is hard on this basis alone to differentiate chemisorption from physisorption.

4.2. Adsorption isotherms

The adsorption of AB dye on MWCM400 (Fig. 9(d)) has been analyzed on the basis of four different adsorption models: (i) the classical Langmuir model [39], (ii) the Freundlich model [40], (iii) the Temkin model [41–43], and (iv) the Dubinin–Radushkevich (D–R) model [44,45]. The Langmuir isotherm is based on the assumptions of constant adsorption energy, freedom from interactions between

Table 1
Kinetic parameters for adsorption of AB dye onto MWCM400

Temperature (°C)	q_{exp} (mg g ⁻¹)	Pseudo-first-order			Pseudo-second-order		
		$10^2 (k_1, \text{h}^{-1})$	q_{calc} (mg g ⁻¹)	r_1	$10^2 (k_2, \text{g mg}^{-1} \text{h}^{-1})$	q_{calc} (mg g ⁻¹)	r_2
25	29.54	2.4	17.05	0.9895	0.8	29.32	0.9992
45	29.56	7.9	17.62	0.9730	2.4	29.99	0.9997
65	32.45	26.1	23.97	0.9579	5.9	27.72	0.9897

Note: Initial AB dye concentration, $C_0 = 600 \text{ mg L}^{-1}$.

neighboring adsorbed species, a homogeneous adsorbent surface, and adsorption limited to a monolayer [46]. By contrast, the Freundlich model is essentially empirical, yielding an equation based on the assumption that adsorption takes place not on a homogeneous, but on a heterogeneous surface [47], whereas the Temkin model supposes that the heat of adsorption of all molecules in a layer decreases linearly with coverage as a result of the adsorbent–adsorbate interactions. The D–R isotherm is based on a model more general than the Langmuir one; postulating neither a homogeneous surface nor a constant adsorption potential, it expresses the adsorption mechanism with a Gaussian energy distribution on a heterogeneous surface. Each model can be expressed in the form of an appropriate linearized equation which has been applied to the present experimental results (Table 2).

With values of r consistently closest to 1, the Langmuir model appears best to accommodate the experimental results at the three temperatures studied. This is consistent with an adsorption process involving relatively weak, non-specific AB dye-MWCM400 interactions and adsorbed species relatively well dispersed on the surface of the adsorbent.

4.3. Thermodynamic parameters

The enthalpy change, $\Delta H_{\text{ads}}^\circ$, and entropy change, $\Delta S_{\text{ads}}^\circ$, attending the adsorption process have been estimated via the van't Hoff equation [44]:

$$\ln K_L = -\frac{\Delta H_{\text{ads}}^\circ}{RT} + \frac{\Delta S_{\text{ads}}^\circ}{R} \quad (4)$$

where K_L is the equilibrium constant obtained from the Langmuir isotherm. The plot of $\ln K_L$ vs. T^{-1} gives a straight line with a slope $-\Delta H_{\text{ads}}^\circ/R$ and intercept $\Delta S_{\text{ads}}^\circ/R$, while $\Delta G_{\text{ads}}^\circ$ is accessible via Eq. (5):

$$\Delta G_{\text{ads}}^\circ = -RT \ln K_L \quad (5)$$

Table 2
Isotherm parameters for the adsorption of AB dye onto MWCM400 at 25, 45, and 65 °C

Isotherms	Temperature (°C)		
	25	45	65
<i>Langmuir</i>			
K_L (L g ⁻¹) ^a	0.050	0.097	1.083
Q_m (mg g ⁻¹) ^b	74.24	71.63	97.18
r^c	0.9949	0.98727	0.9924
<i>Freundlich</i>			
K_F (mg g ⁻¹ or mg ⁿ g ⁻ⁿ) ^d	0.0007	0.054	0.025
n^e	0.334	0.551	0.467
r^c	0.9055	0.9289	0.9722
<i>Temkin</i>			
A (L g ⁻¹) ^f	1.559	0.274	0.3114
b^g	226.58	136.11	175.65
r^c	0.9944	0.9357	0.8960
<i>Dubinin–Radushkevich</i>			
β (10 ⁻⁶) ^h	1.49	6.28	2.62
Q_{DR} (mg g ⁻¹) ⁱ	52.32	53.34	53.51
r^c	0.7569	0.6243	0.5599

^aLangmuir constant.

^bMaximum adsorption capacity of the adsorbent for the dye.

^cLinear regression coefficient.

^dFreundlich constant.

^eEmpirical parameter related to the adsorption “intensity”.

^fTemkin constant.

^gConstant related to the heat of adsorption.

^hConstant related to the mean free energy of adsorption per mole of the adsorbate.

ⁱTheoretical saturation capacity.

The values found for $\Delta H_{\text{ads}}^\circ$ and $\Delta S_{\text{ads}}^\circ$ are +64 kJ mol⁻¹ and +186 J K⁻¹ mol⁻¹, respectively, while $\Delta G_{\text{ads}}^\circ$ varies from +7.43, through +6.17, to -0.22 kJ mol⁻¹ at 25, 45, and 65 °C, respectively. The process is plainly endothermic and driven by the overall increase in randomness that occurs at the solid/solution interface during adsorption. The values of $\Delta G_{\text{ads}}^\circ$, which

Table 3

Comparison of different adsorbents/biosorbents for adsorption of AB dye and other adsorbates from aqueous solution at 20–30°C

Sorbent	Temperature (°C)	Q_{\max} (mg g ⁻¹)	Refs.
Biomass of Baker's yeast	30	70.00	[56]
Commercial activated carbon	30	18.50	[56]
Green macroalga <i>Caulerpa lentillifera</i>	25	94.34	[57]
Macroalga <i>Caulerpa lentillifera</i>	25	38.90	[58]
Fly ash	30	128.21	[15]
Sepiolite	20	312.50	[36]
MWCM400	25	74.24	This study

decrease with increasing temperature, show the process to be a non-spontaneous one at lower temperatures, but to become narrowly spontaneous at 65°C [48].

4.4. Activation energy

The Arrhenius equation (Eq. (6)) gives access to the activation energy for adsorption of AB dye onto MWCM400 [49]:

$$\ln k_2 = \ln A - \frac{E_a}{RT} \quad (6)$$

where A is the frequency factor (g mg⁻¹ h⁻¹) and E_a the activation energy of the adsorption process (kJ mol⁻¹). A plot of $\ln k_2$ vs. T^{-1} takes the form of a straight line with a gradient $-E_a/R$. In principle, the activation energy provides information about the nature of the adsorption. Physisorption through Coulombic and dispersion forces is typically characterized by values of E_a in the range 5–40 kJ mol⁻¹: chemisorption, in which covalent forces play a significant part, is more likely to feature E_a values in the range 40–800 kJ mol⁻¹. In the event, the Arrhenius plot affords an E_a value of 9.5 kJ mol⁻¹ for the adsorption of AB dye by MWCM400, indicating the sort of potential barrier that is usually associated with physisorption. This involves presumably (i) Coulombic interaction between negatively charged groups on the adsorbent surface (CO₃²⁻, SO₄²⁻, and O²⁻) and the cations of the AB dye [50]; (ii) interaction between the transient dipoles induced in the π -charge clouds of the aromatic rings and $-N=N-$ or $-N=C-C=C-$ functionalities of the dye and the negatively charged MWCM400 surface [51]; and (iii) hydrogen bonding between OH groups on the material surface and electron-rich sites of the dye [52].

4.5. Comparison of adsorbents

Comparison of the adsorption capacities of various types of adsorbent or biosorbent for AB dye in aqueous solution (Table 3) shows that MWCM400 has a capacity for this dye that compares favorably with those of the other adsorbents or biosorbents listed, being bettered by only two of them. Numerous studies along similar lines have been carried out with varying degrees of success with agents such as activated carbon [53], pomelo peels [54], Gondwana shale [55], and Rambutan seed [37] as adsorbents for dyestuffs such as Malachite green [37,53,54] or aromatics such as phenol [55] in aqueous media. In view of its easy availability and low cost, as well as the desirability of reducing the steady accumulation of the parent waste, MWCM400 seems, however, to be worthy of consideration as a non-conventional adsorbent for the treatment of wastewater containing basic dyes.

5. Conclusions

The present study has involved a batch-technique investigation of the adsorption of AB dye from aqueous media by the action of a calcinated fraction of mineral waste from coal mining, MWCM, composed mainly of calcite, dolomite and gypsum. All three of these materials, severally or in combination with other agents, are well known to have significant capacity as adsorbents. Calcite has been used, for example, for the adsorption of metal ions [59,60], as well as phosphate [61] and fluoride [62] from aqueous media. Dolomite, likewise, has been shown to be effective for the removal of not only metal ions [63,64] and phosphate [65], but other polluting agents as well [66], and gypsum has been proposed as a low-cost adsorbent, *inter alia*, for the removal of methylene blue [67] and Reactive Red 1 dye [68] from aqueous solution.

The optimum performance for adsorption of AB dye exhibited by MWCM pre-calcinated at 400°C (MWCM400) reveals that this material is a potential adsorbent of ready local availability and low cost for cationic dye removal from residual waters.

Acknowledgments

The authors are grateful to Capes and CNPq for financial support. They also thank Drs F. Mariani and D.A.M. Zaia, for EDS and FTIR analyses of the samples.

References

- [1] N.F. Cardoso, E.C. Lima, I.S. Pinto, C.V. Amavisca, B. Royer, R.B. Pinto, W.S. Alencar, S.F.P. Pereira, Application of cupuassu shell as biosorbent for the removal of textile dyes from aqueous solution, *J. Environ. Manage.* 92(4) (2011) 1237–1247.
- [2] R. Liu, B. Zhang, D. Mei, H. Zhang, J. Liu, Adsorption of methyl violet from aqueous solution by halloysite nanotubes, *Desalination* 268(1–3) (2011) 111–116.
- [3] M. Roulia, A.A. Vassiliadis, Sorption characterization of a cationic dye retained by clays and perlite, *Microporous Mesoporous Mater.* 116(1–3) (2008) 732–740.
- [4] V. Vimonses, S. Lei, B. Jin, C.W.K. Chow, C. Saint, Adsorption of congo red by three Australian kaolins, *Appl. Clay Sci.* 43(3–4) (2009) 465–472.
- [5] S.S. Moghaddam, M.R.A. Moghaddam, M. Arami, Coagulation/flocculation process for dye removal using sludge from water treatment plant: Optimization through response surface methodology, *J. Hazard. Mater.* 175(1–3) (2010) 651–657.
- [6] C. Fersi, L. Gzara, M. Dhahbi, Flux decline study for textile wastewater treatment by membrane processes, *Desalination* 244(1–3) (2009) 321–332.
- [7] P. Kariyajanavar, N. Jogtappa, Y.A. Nayaka, Studies on degradation of reactive textile dyes solution by electrochemical method, *J. Hazard. Mater.* 190(1–3) (2011) 952–961.
- [8] Y. He, X. Wang, J. Xu, J. Yan, Q. Ge, X. Gu, L. Jian, Application of integrated ozone biological aerated filters and membrane filtration in water reuse of textile effluents, *Bioresour. Technol.* 133 (2013) 150–157.
- [9] U.F. Alkaram, A.A. Mukhlis, A.H. Al-Dujaili, The removal of phenol from aqueous solutions by adsorption using surfactant-modified bentonite and kaolinite, *J. Hazard. Mater.* 169(1–3) (2009) 324–332.
- [10] C.A.P. Almeida, N.A. Debacher, A.J. Downs, L. Cottet, C.A.D. Mello, Removal of methylene blue from colored effluents by adsorption on montmorillonite clay, *J. Colloid Interface Sci.* 332(1) (2009) 46–53.
- [11] C.A.P. Almeida, A. dos Santos, S. Jaeger, N.A. Debacher, N.P. Hankins, Mineral waste from coal mining for removal of astrazon red dye from aqueous solutions, *Desalination* 264(3) (2010) 181–187.
- [12] D.L. Guerra, R.R. Viana, C. Airoidi, Adsorption of thorium cation on modified clays MTTZ derivative, *J. Hazard. Mater.* 168(2–3) (2009) 1504–1511.
- [13] M.H. Kalavathy, L.M. Miranda, *Moringa oleifera*—A solid phase extractant for the removal of copper, nickel and zinc from aqueous solutions, *Chem. Eng. J.* 158(2) (2010) 188–199.
- [14] S. Lei, V. Vimonses, B. Jin, C.W.K. Chow, C. Saint, Kinetic study and equilibrium isotherm analysis of Congo Red adsorption by clay materials, *Chem. Eng. J.* 148(2–3) (2010) 354–364.
- [15] B. Karagozolu, M. Tasdemir, E. Demirbas, M. Kobya, The adsorption of basic dye (Astrazon Blue FGRL) from aqueous solutions onto sepiolite, fly ash and apricot shell activated carbon: Kinetic and equilibrium studies, *J. Hazard. Mater.* 147(1–2) (2007) 297–306.
- [16] H.P. Boehm, Some aspects of the surface chemistry of carbon blacks and other carbons, *Carbon* 32(5) (1994) 759–769.
- [17] A. Çelekli, M. Yavuzatmaca, H. Bozkurt, An eco-friendly process: Predictive modelling of copper adsorption from aqueous solution on *Spirulina platensis*, *J. Hazard. Mater.* 173(1–3) (2010) 123–129.
- [18] L.M. Correia, N.S. de Sousa Campelo, D.S. Novaes, C.L. Cavalcante Jr., J.A. Cecilia, E. Rodríguez-Castellón, R.S. Vieira, Characterization and application of dolomite as catalytic precursor for canola and sunflower oils for biodiesel production, *Chem. Eng. J.* 269 (2015) 35–43.
- [19] R. Marouf, K. Marouf-Khelifa, J. Schott, A. Khelifa, Zeta potential study of thermally treated dolomite samples in electrolyte solutions, *Microporous Mesoporous Mater.* 122(1–3) (2009) 99–104.
- [20] J. Wang, D. Yu, X. Zeng, J. Chen, M. Si, C. Wen, M. Xu, Effect of carbon dioxide on the high temperature transformation of siderite under low oxygen conditions, *Fuel* 148 (2015) 73–78.
- [21] L.M. Correia, R.M.A. Saboya, N.S. de Sousa Campelo, J.A. Cecilia, E. Rodríguez-Castellón, C.L. Cavalcante Jr., Characterization of calcium oxide catalysts from natural sources and their application in the transesterification of sunflower oil, *Bioresour. Technol.* 151 (2014) 207–213.
- [22] A. Putnis, B. Winkler, L. Fernandez-Diaz, In situ IR spectroscopic and thermogravimetric study of the dehydration of Gypsum, *Mineral. Mag.* 54(374) (1990) 123–128.
- [23] M. Lazón, P.A. García-Ruiz, Effect of acid setting inhibition and mechanical properties of gypsum buildin plasters, *Constr. Build Mater.* 28(1) (2012) 506–511.
- [24] L. Tourneret, F. Berger, C. Mavon, A. Chambaudet, Calcium sulphate formation during the heat-up period: Some essential parameters, *Appl. Clay Sci.* 14(5–6) (1999) 299–317.
- [25] S.J. Gregg, K.S.W. Sing, Adsorption, Surface Area and Porosity, second ed., Academic Press, London, 1982.
- [26] A.M. Oickle, S.L. Goertzen, K.R. Hopper, Y.O. Abdalla, H.A. Andreas, Standardization of the Boehm titration: Part II. Method of agitation, effect of filtering and dilute titrant, *Carbon* 48(12) (2010) 3313–3322.
- [27] M.-H. Baek, C.O. Ijagbemi, S.-J.O.D.-S. Kim, Removal of Malachite Green from aqueous solution using degreased coffee bean, *J. Hazard. Mater.* 176(1–3) (2010) 820–828.
- [28] S. Chen, J. Zhang, C. Zhang, Q. Yue, Y. Li, C. Li, Equilibrium and kinetic studies of methyl orange and methyl violet adsorption on activated carbon derived from *Phragmites australis*, *Desalination* 252(1–3) (2010) 149–156.

- [29] Ç. Doğar, A. Gürses, M. Açıkıldız, E. Özkan, Thermodynamics and kinetic studies of biosorption of a basic dye from aqueous solution using green algae *Ulothrix* sp., *Colloids Surf., B* 76(1) (2010) 279–285.
- [30] N. Nasuha, B.H. Hameed, A.Y.M. Din, Rejected tea as a potential low-cost adsorbent for the removal of methylene blue, *J. Hazard. Mater.* 175(1–3) (2010) 126–132.
- [31] O. Hamdaoui, Batch study of liquid-phase adsorption of methylene blue using cedar sawdust and crushed brick, *J. Hazard. Mater.* 135(1–3) (2006) 264–273.
- [32] S. Lagergren, About the theory of so-called adsorption of soluble substances, *Kungliga Svenska Vetenskapsakademiens Handlingar* 24(4) (1898) 1–39.
- [33] Y.S. Ho, G. McKay, Sorption of dye from aqueous solution by peat, *Chem. Eng. J.* 70(2) (1998) 115–124.
- [34] Y.S. Ho, G. McKay, The kinetics of sorption of divalent metal ions onto sphagnum moss peat, *Water Res.* 34(3) (2000) 735–742.
- [35] Y.S. Ho, Comment on “Selective adsorption of tannins onto hide collagen fibres”, *Sci. China Ser. B* 48(2) (2005) 176.
- [36] A. Ongen, H.K. Ozcan, E.E. Ozbas, N. Balkaya, Adsorption of Astrazon Blue FGRL onto sepiolite from aqueous solutions, *Desalin. Water Treat.* 40 (2012) 129–136.
- [37] M.A. Ahmad, N.S. Afandi, K.A. Adegoke, O.S. Bello, Optimization and batch studies on adsorption of malachite green dye using rambutan seed activated carbon, *Desalin. Water Treat.* (in press), doi: 10.1080/19443994.2015.1119744.
- [38] S. Chowdhury, S. Chakraborty, P. Saha, Biosorption of Basic Green 4 from aqueous solution by *Ananas comosus* (pineapple) leaf powder, *Colloids Surf., B* 84(2) (2011) 520–527.
- [39] I. Langmuir, The constitution and fundamental properties of solids and liquids. Part I. Solids, *J. Am. Chem. Soc.* 38(11) (1916) 2221–2295.
- [40] H.M.F. Freundlich, About the adsorption in solution, *J. Phys. Chem.* 57(A) (1906) 385–470.
- [41] G.O. El-Sayed, Removal of methylene blue and crystal violet from aqueous solutions by palm kernel fiber, *Desalination* 272(1–3) (2011) 225–232.
- [42] N.M. Mahmoodi, B. Hayati, M. Arami, C. Lan, Adsorption of textile dyes on Pine Cone from colored wastewater: Kinetic, equilibrium and thermodynamic studies, *Desalination* 268(1–3) (2011) 117–125.
- [43] H. Runping, H. Pan, C. Zhaohui, Z. Zhenhui, T. Mingsheng, Kinetics and isotherms of Neutral Red adsorption on peanut husk, *J. Environ. Sci.* 20(9) (2008) 1035–1041.
- [44] P.W. Atkins, J. de Paula, *Physical Chemistry*, eighth ed., Oxford University Press, Oxford, 2006.
- [45] A.S. Özcan, B. Erdem, A. Özcan, Adsorption of Acid Blue 193 from aqueous solutions onto BTMA-bentonite, *Colloids Surf., A* 266(1–3) (2005) 73–81.
- [46] C.A.P. Almeida, C. Machado, N.A. Debacher, Adsorption of methylene blue as a model for the use of Barro Branco as an alternative adsorbent for color removal, *Progr. Colloid Polym. Sci.* 128 (2004) 278–282.
- [47] R. Arasteh, M. Masoumi, A.M. Rashidi, L. Moradi, V. Samimi, S.T. Mostafavi, Adsorption of 2-nitrophenol by multi-wall carbon nanotubes from aqueous solutions, *Appl. Surf. Sci.* 256(14) (2010) 4447–4455.
- [48] R.M. Schneider, C.F. Cavalin, M.A.S.D. Barros, C.R.G. Tavares, Adsorption of chromium ions in activated carbon, *Chem. Eng. J.* 132(1–3) (2007) 355–362.
- [49] E. Eren, O. Cubuk, H. Ciftci, B. Eren, B. Caglar, Adsorption of basic dye from aqueous solutions by modified sepiolite: Equilibrium, kinetics and thermodynamics study, *Desalination* 252(1–3) (2010) 88–96.
- [50] X. Liu, X. Lu, M. Sprik, J. Cheng, E.J. Meijer, R. Wang, Acidity of edge surface sites of montmorillonite and kaolinite, *Geochim. Cosmochim. Acta* 117 (2013) 180–190.
- [51] M.F.R. Pereira, S.F. Soares, J.J.M. Órfão, J.L. Figueiredo, Adsorption of dyes on activated carbons: Influence of surface chemical groups, *Carbon* 41(4) (2003) 811–821.
- [52] D. Tunega, G. Haberhauer, M.H. Gerzabek, H. Lischka, Theoretical study of adsorption sites on the (0 0 1) surfaces of 1:1 clay minerals, *Langmuir* 18(1) (2002) 139–147.
- [53] O.S. Bello, M.A. Ahmad, N. Ahmad, Adsorptive features of banana (*Musa paradisiaca*) stalk-based activated carbon for malachite green dye removal, *Chem. Ecol.* 28 (2012) 153–167.
- [54] O.S. Bello, M.A. Ahmad, B. Semire, Scavenging malachite green dye from aqueous solutions using pomelo (*Citrus grandis*) peels: Kinetic, equilibrium and thermodynamic studies, *Desalin. Water Treat.* 56 (2015) 521–535.
- [55] K. Sadhu, A. Mukherjee, S.K. Shukla, K. Adhikari, S. Dutta, Adsorptive removal of phenol from coke-oven wastewater using Gondwana shale, India: Experiment, modeling and optimization, *Desalin. Water Treat.* 52 (2014) 6492–6504.
- [56] J.Y. Farah, N.S. El-Gendy, L.A. Farahat, Biosorption of Astrazone Blue basic dye from an aqueous solution using dried biomass of Baker’s yeast, *J. Hazard. Mater.* 148(1–2) (2007) 402–408.
- [57] P. Punjorharn, K. Meevasana, P. Pavasant, Influence of particle size and salinity on adsorption of basic dyes by agricultural waste: Dried Seagrass (*Caulerpa lentillifera*), *J. Environ. Sci.* 20(6) (2008) 760–768.
- [58] K. Marungrueng, P. Pavasant, Removal of basic dye (Astrazon Blue FGRL) using macroalga *Caulerpa lentillifera*, *J. Environ. Manage.* 78(3) (2006) 268–274.
- [59] H. Merrikpour, M. Jalali, Waste calcite sludge as an adsorbent for the removal of cadmium, copper, lead and zinc from aqueous solutions, *Clean Technol. Environ. Policy* 14(5) (2012) 845–855.
- [60] K. Song, W. Kim, T. Ryu, K.-W. Ryu, J.-H. Bang, Y.-N. Jang, Adsorption of Cd(II) on waste calcite produced by the carbonation of flue gas desulfurization (FGD) gypsum, *Mater. Trans.* 52(2) (2011) 224–228.
- [61] K. Karageorgiou, M. Paschalis, G.N. Anastassakis, Removal of phosphate species from solution by adsorption onto calcite used as natural adsorbent, *J. Hazard. Mater.* 139(3) (2007) 447–452.
- [62] M. Poonam, G. Suja, M. Dhiraj, Use of calcite for defluoridation of drinking water in acidic medium, *Res. J. Chem. Sci.* 4(6) (2014) 62–65.
- [63] A.B. Albadarin, C. Mangwandi, A.H. Al-Muhtaseb, G.M. Walker, S.J. Allen, M.N.M. Ahmad, Kinetic and thermodynamics of chromium ions adsorption onto low-cost dolomite adsorbent, *Chem. Eng. J.* 179 (2012) 193–202.

- [64] S. Kocaoba, Comparison of Amberlite IR 120 and dolomite's performances for removal of heavy metals, *J. Hazard. Mater.* 147(1–2) (2007) 488–496.
- [65] S. Karaca, A. Gurses, M. Ejder, M. Acikyildiz, Adsorptive removal of phosphate from aqueous solutions using raw and calcinated dolomite, *J. Hazard. Mater.* 128(2–3) (2006) 273–279.
- [66] E. Escamilla-Roa, C.I. Sainz-Díaz, F.J. Huertas, A. Hernández-Laguna, Adsorption of molecules onto (1014) dolomite surface: An application of computational studies for microcalorimetry, *J. Phys. Chem. C* 117(34) (2013) 17583–17590.
- [67] M.A. Rauf, I. Shehadeh, A. Ahmed, A. Al-Zamly, Removal of Methylene Blue from aqueous solution by using gypsum as a low cost adsorbent, *World Acad. Sci.: Eng. Technol.* 3 (2009) 540–545.
- [68] C.C. Obunwo, I. Ubong, G.I. Orgu, Removal of Reactive Red 1 dye from aqueous solution using gypsum, *Int. J. Biol. Chem. Sci.* 6 (2012) 2202–2210.